



848 ppi high-brightness active-matrix micro-LED micro-display using GaN-on-Si epi-wafers towards mass production

LONGHENG QI,  XU ZHANG,  WING CHEUNG CHONG,  PEIAN LI, AND KEI MAY LAU* 

Photonics Technology Center, Department of Electronic and Computer Engineering, The Hong Kong University of Science and Technology, Clear Water Bay, Hong Kong

*eekm lau@ust.hk

Abstract: In this paper, fabrication processes of a 0.55-inch 400×240 high-brightness active-matrix micro-light-emitting diode (LED) display using GaN-on-Si epi-wafers are described. The micro-LED array, featuring a pixel size of $20 \mu\text{m} \times 20 \mu\text{m}$ and a pixel density of 848 pixels per inch (ppi), was fabricated and integrated with a custom-designed CMOS driver through Au-Sn flip-chip bonding. Si growth substrate was removed using a crack-free wet etching method. Four-bit grayscale images and videos are clearly rendered. Optical crosstalk is discussed and can be mitigated through micro-LED array design and process modification. This high-performance, high-resolution micro-LED display demonstration provides a promising and cost-effective solution towards mass production of micro-displays for VR/AR applications.

© 2021 Optical Society of America under the terms of the [OSA Open Access Publishing Agreement](#)

1. Introduction

Micro-LED technology has received a great deal of attention due to its various promising applications in high modulation bandwidth visible light communication (VLC) [1–3], neuron stimulation, optogenetic sources [4–6] and micro-display [7–9]. For micro-display applications such as projectors and near-to-eye (NTE) displays including augmented reality (AR) [10,11], virtual reality (VR), and wearable devices, micro-LED is the most promising solution in current mainstream display technologies. Compared to liquid crystal displays (LCDs), micro-LEDs are self-emissive devices, which can provide much higher contrast and efficiency, leading to lower power consumption and longer battery lifetime of the whole system. While organic light-emitting diodes (OLEDs) can also achieve self-emissive display, they suffer from stability, lifetime and brightness issues, especially under a high driving current. By contrast, micro-LED displays based on GaN/InGaN, an inorganic semiconductor material, show a much longer lifespan and robustness, even under extreme conditions, and provide much higher brightness than OLED displays [12]. Furthermore, micro-LED display chips can be directly fabricated on a single III-nitride epi-wafer grown on Si substrates using conventional microelectronic processing methods and equipment, to achieve high resolution for hybrid integration with the CMOS driver.

Micro-LED displays based on GaN-on-sapphire epi-wafers have been heavily researched during the past decade. Our group has successfully demonstrated a 60×60 active-matrix [13] and a 256×192 passive-matrix [14] micro-LED display using LED on sapphire substrates in 2013 and 2014, respectively. Later, a 400×240 active-matrix driven micro-LED display with VLC function was developed [15]. Day et al. [16,17] reported the first VGA resolution (640×480) green InGaN active-matrix display, which had a pixel size of $12 \mu\text{m}$ and a pixel pitch of $15 \mu\text{m}$. Further, Templier et al. [18,19] developed an active-matrix blue micro-LED display with a resolution of 873×500 and a pixel pitch down to $10 \mu\text{m}$. The pixel brightness could reach up to millions of nits (cd/m^2), but no panel brightness data was given. In 2019, Chen et al. [20] demonstrated an active-matrix-driven micro-LED display with a resolution as high as 960×540 ,

and a pixel size of 8 μm . The above works show the potential of high-resolution micro-LED displays using sapphire substrate and their promising application in projectors and NTE displays. Using GaN-on-sapphire epi-wafers for micro-LED array fabrication for micro-displays may not be the most favorable for volume production. First, to overcome the severe optical crosstalk issue induced by sapphire, a costly laser lift-off (LLO) process that may compromise the performance of the LED array is required to remove the sapphire substrate. Second, the size of sapphire substrate for GaN growth is much smaller compared to that of Si substrates. The maximum size of Si substrate used in the conventional microelectronics industry is as large as 12 inches. Therefore, fabricating a micro-LED display chip on a GaN-on-Si epi-wafer can be more cost-effective, especially with the continuous improvement of GaN-on-Si epitaxy technology. Some companies have made progress in large-scale GaN-on-Si epitaxy growth [21] and high-density micro-LEDs process using wafer-level bonding [22].

Previously, our group demonstrated a Cu-Sn flip-chip bonded GaN-on-Si active-matrix driven micro-LED display prototype with a resolution of 64×36 [23]. In this paper, a much higher resolution (400×240) active-matrix micro-LED display using GaN-on-Si epi-wafers was designed, fabricated, and demonstrated. The display, adopting a robust Au-Sn bonding scheme, features a pixel size of 20 μm and a pixel pitch of 30 μm within a display diagonal of 0.55 inches, reaching a high pixel density of 848 ppi. The pixel size and pitch are defined by the mask design but limited by the performance of equipment used for fabrication, such as the photomask aligner and flip-chip bonder. Definitely, using this monolithic fabrication method, the pixel size can be scaled down further leading to higher display resolution if high-performance equipment are applied. The bowing and cracking issue of GaN thin film induced by thermal mismatch during Si substrate removal was addressed in this work. This high-resolution GaN-on-Si micro-LED display shows a maximum brightness of up to 8300 cd/m^2 under full-load condition.

The remainder of this paper is divided into four sections. Section II discusses the design and fabrication details of the GaN-on-Si micro-LED array. Section III presents the measurement results of this micro-display system, including pixel level and panel level characterizations, as well as the display demonstration. Discussion on optical crosstalk is also given. Finally, conclusions are drawn in Section IV.

2. Experiments

Commercial 4-inch GaN-on-Si epi-wafers with a typical blue LED epi-structure grown by metal-organic chemical vapor deposition (MOCVD) were used for fabrication of the micro-LED arrays. The LED epi-structure consists of a 1.35 μm -thick AlGaIn buffer layer, 1.2 μm -thick n-type GaN layer, and 12 blue InGaIn/GaN multiple quantum wells (MQWs) totaling 180 nm-thick, followed by a 160 nm p-type GaN layer on top. The threading dislocation density is estimated to be $1 \times 10^8 \text{ cm}^{-2}$. To start with, a layer of 115 nm-thick indium tin oxide (ITO) was deposited as a current spreading layer by E-beam evaporation. Then each micro-LED pixel, with a pitch size of 30 μm , was patterned by ITO wet etching in dilute aqua regia using photoresist as an etching mask. The mesa structure of each micro-LED pixel is self-aligned to the patterned ITO and formed by inductively coupled plasma (ICP) etching, to a size of 20 $\mu\text{m} \times 20 \mu\text{m}$. An additional diluted aqua regia cleaning was treated to eliminate possible leakage current paths resulting from ITO particles on the sidewalls induced by dry etching. Annealing process was performed in O_2 and N_2 ambience, at 600°C and 750°C for 5 min and 30 s respectively, to optimize the transparency and conductivity of the ITO. A Cr/Al-based multi-metal layer was then deposited on the ITO layer and n-GaN as p- and n-electrodes, respectively, as shown in Fig. 1(a). The individual p-electrode covers the whole ITO layer and serves as a light mirror in this bottom-emitting structure after flip-chip bonding. The common n-electrode was designed as a grid structure, thus reducing the number of bonding pads while providing uniform current flow to each micro-LED pixel for uniform light output. The mesa sidewalls of each micro-LED pixel were passivated by a

layer of SiO₂ using plasma-enhanced chemical vapor deposition (PECVD) to reduce the current leakage caused by dry etching damage and defects. Next, another transparent high-temperature overcoat photoresist was spin coated to planarize the surface, followed by contact holes opening and Sn deposition, as depicted in Fig. 1(b). Figure 1(c) demonstrates the micro-LED array morphology after Sn reflow. Deposited Sn pads were turned into spherical bumps with the help of flux by a three-stage reflow process. The deoxidation stage was firstly performed in formic gas ambience at 200°C for 30 s, then a premelting stage was performed at 220°C for 10 s, followed by a 5 s quick reflow step. The heights of the p-bumps and n-bumps are around 9 μm and 7 μm, respectively. Finally, the micro-LED chip was flip-chip bonded onto the CMOS backplane by Sn solder bumps and Au pads on each pixel and pixel driver contacts. The cross-section in Fig. 1(d) shows the robust connection of the micro-LED chip and CMOS backplane. An appropriate proportion of hydrofluoric-nitric-acetic (HNA) mixed solution was used for (111) Si substrate etching at etching rates of 17 ~ 20 μm/min and anti-corrosion underfill was used as a protective layer of peripheral and bottom Si CMOS circuits. To address the bowing and cracking issue of GaN thin film induced by thermal stress during Si removal, mechanically and thermally stable Au-Sn bonding and heatless wet etching process were performed. Compared to the SF₆-based plasma dry etching method [23], wet etching can significantly reduce heat generation during substrate removal, avoiding GaN film bowing and cracking over such a large-size display chip. This method is also more time-efficient, generally reducing etching time from hours to minutes but meanwhile providing better etching uniformity and yield. Figure 1(e) depicts the hybrid chip surface after Si growth substrate removal, exposing a transparent and crack-free GaN buffer layer. To drive this GaN-on-Si micro-LED display chip, the chip was wire-bonded onto the

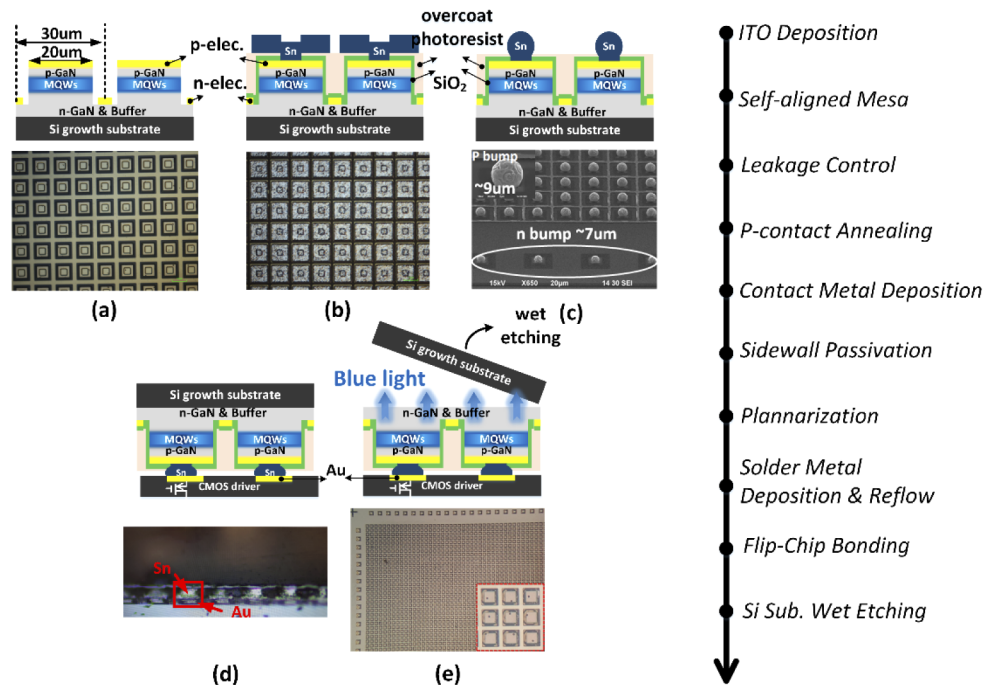


Fig. 1. Process flow of active-matrix GaN-on-Si micro-LED display and corresponding process inspections: (a) after mesa formation and p-n junction stack deposition, (b) after sidewall passivation, surface planarization, via opening and tin deposition, (c) after Sn pads reflow into Sn ball-shaped bumps, (d) after flip-chip bonding of micro-LED array and CMOS driver and the corresponding SEM cross-section, and (e) after Si growth substrate removal.

daughterboard and connected to an FPGA controlling motherboard through a flexible cable. The motherboard processes and delivers display data to the on-chip column drivers, and updates the images/videos on the micro-LED display panel accordingly. The frame rate of this micro-LED display is 10 when displaying video content.

3. Results

3.1. Pixel-level characterization

Our flip-chip bottom emission configuration of micro-displays requires optical measurements to be performed after the flip-chip bonding and Si growth substrate removal. Before flip-chip bonding, single-pixel electrical characteristics were measured by a probe station. Figure 2(a) shows the current-voltage (I - V) characteristics of a single pixel. The reverse saturation current is around 5 pA at a bias of -5 V, showing a low leakage current and large shunt resistance R_p of hundreds of giga-Ohms. The ideality factor n and series resistance R_s can be therefore extracted by ignoring the shunt resistance at forward bias through the equation,

$$I \frac{dV}{dI} = IR_s + n \frac{kT}{q} \quad (1)$$

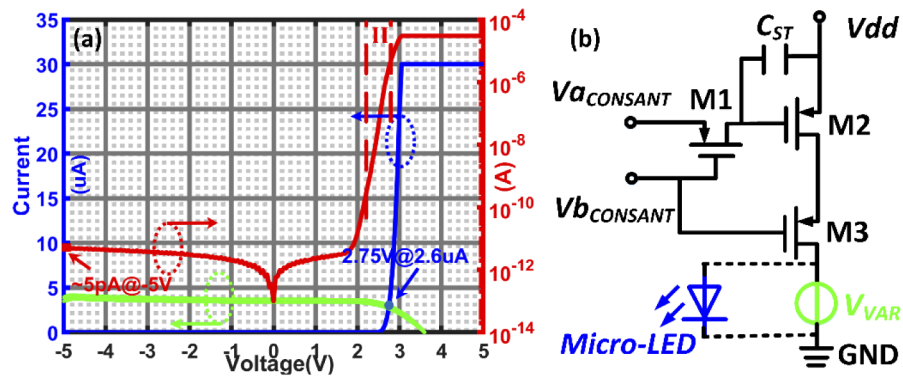


Fig. 2. (a) Single micro-LED pixel I - V characteristic in log scale (red) and linear scale (blue), and pixel driver output curve (green) under half-load condition (The pixel is measured before flip-chip bonding and after Sn reflow process). (b) Measurement schematic of pixel driver driving capability.

Ideality factor n at region II ($2.1 \text{ V} < V < 2.9 \text{ V}$) [24] (logarithm scale) was extracted to be 1.63 and R_s is 5.5 k Ω . The low ideality factor in this region indicates the dominant radiative recombination and low carrier leakage [25] resulting from few defects and sidewall treatment of the improved process. The increase of ideality factor caused by current crowding effect is also suppressed in this quasi-vertical micro-LED structure with grid-like common n-electrodes design. To define the forward voltage of the micro-LED pixel, we assume the display operates at 50% of the maximum brightness under normal operation condition. Therefore, the pixel driver output curve was measured at half-load condition which corresponds to the half brightness of the maximum brightness of a single pixel. The measurement schematic is shown in Fig. 2(b). Port ' V_a ' and ' V_b ' were set at constant voltages to ensure the on-state of M1, M2 and M3. ' V_{dd} ' was pulled to a high voltage level to provide power. Micro-LED pixel was open-circuit and replaced by a variable voltage source. Then the current flowing through is the measured output current of the pixel driver. The operation point of micro-LED pixels occurs at the intersection of the pixel driver output curve and pixel I - V curve (linear scale), which is around 2.6 μA , as shown in

Fig. 2(a). The corresponding voltage at this operation point is defined at the forward voltage of 2.75 V.

3.2. Panel-level characterization

In addition to the electrical characterization of a single pixel, the micro-LED array was also analyzed at the panel level to demonstrate the display performance. As shown in Fig. 3(a), a clear and flat GaN thin film is exposed after flip-chip bonding and Si substrate removal, indicating the uniform and crack-free wet etching. The chip size of the micro-LED display is 17.1 mm × 10.1 mm and the display area is 12 mm × 7.2 mm, in which the total active area is 0.384 cm². Figure 3(b) shows a photo of the GaN-on-Si micro-LED display when all the pixels (96,000) are turned-on at a driving current of 200 mA. To estimate the pixel yield, regions were randomly picked over the 0.55 inches display region, each of which contains 20 × 20 pixels. The average yield is larger than 95%. As a matter of fact, one of the most significant issues that needs to be taken into consideration for micro-LED display development and commercialization is the yield issue. Bonding and substrate removal are the key factors for the yield improvement of this GaN-on-Si monolithic micro-LED display chip. In our experiments, yield will be further improved if less contamination could be controlled during the fabrication process and the design of Sn pads is optimized, as dead pixels are primarily caused by Sn pads damage and solder bumps reflow failure before flip-chip bonding and substrate removal. The inset of Fig. 3(b) shows the uniform light output of each pixel in the array, which is contributed by the robust Au-Sn bonding and grid-like common n-electrodes design. No evident current-dependent non-uniformity was observed at the currents near and above the pixel operation point.

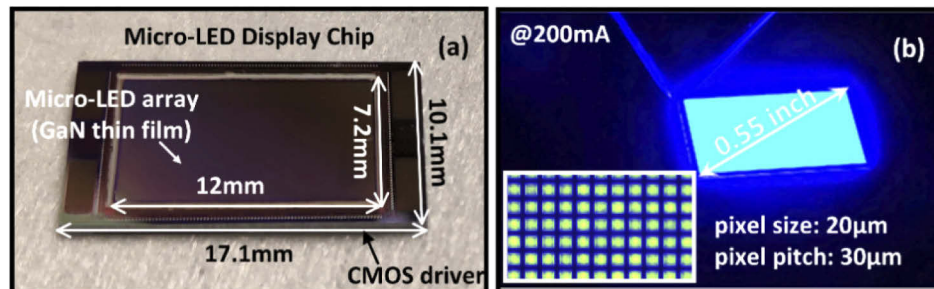


Fig. 3. (a) Display chip image after micro-LED array flip-chip bonded onto CMOS driver and Si growth substrate removal. (b) The Micro-LED display chip was powered by 200 mA DC using a probe station, showing high yield and uniform light output. The inset shows the magnification image of the powered-on pixel array.

The light output power (LOP) and external quantum efficiency (EQE) were measured in an integrating sphere. With current increasing, the LOP of the array increases linearly and shows a maximum value of 146 mW when driving with a DC current of 1 A. The DC measurement can measure up to 1 A or above by directly probing the power rail and ground rail of all the micro-LED pixels on the CMOS driver to further investigate the electrical and optical performance beyond the driving capability of this custom-designed CMOS driver. For the micro-display operating at full-load condition, the maximum current that the CMOS driver can provide is 500 mA. With this injection current, the LOP of the whole array is 54.9 mW (see Fig. 4 black curve). Average pixel EQE, i.e., EQE_{ave} , can be derived from the spectra through integrating the product of each sampling wavelength and corresponding spectral power density divided by the injection current

and a group of physical constants, which is expressed by

$$EQE_{ave} = \frac{\int_{400nm}^{500nm} \lambda_i SPD(\lambda_i) d\lambda_i}{I} \frac{e}{hc} \quad (2)$$

where λ_i is the sampling wavelength from the integrating sphere, $SPD(\lambda_i)$ is the electroluminescence (EL) spectral power density at wavelength λ_i , I represents total injection current. Compared to single-pixel measurement, this global measurement can also reflect the performance of the micro-LED array in display applications more accurately as we consider their operating characteristics in terms of a whole display rather than individual pixels. Figure 4 shows the measured EQE_{ave} (red curve) as a function of current density. No current-related efficiency droop is observed in the measurement range since the current density is relatively low. Daami *et al.* [26], Tian *et al.* [27], and Oliver *et al.* [28] reported the EQE size-dependence of GaN-on-sapphire micro-LEDs, indicating that the EQE common droop limit would shift to larger current density with micro-LED size reduction. According to these reported results and our study, the common efficiency droop limit occurs at a current density larger than 10 A/cm² for micro-LEDs whose sizes are smaller than 50 μ m. For the 20 μ m micro-LED pixel in this display, the maximum EQE_{ave} reaches 4% under full-load condition, corresponding to a current density of 1.35 A/cm². This result is comparable and similar to those reported GaN-on-sapphire micro-LEDs [26–28]. Higher EQE_{ave} can be obtained by driving micro-LED pixels to operate at current density where the common efficiency droop limit occurs, but the system power consumption will become an issue especially for high-resolution display. In this micro-LED display system, the maximum power consumption with all pixels turned-on under full-load condition is around 1.17 W. To enhance the EQE performance, process conditions such as mesa etching parameters, sidewall treatment and passivation materials need to be further optimized [29]. Moreover, fully-vertical micro-LED structure can be considered to improve the current spreading [30].

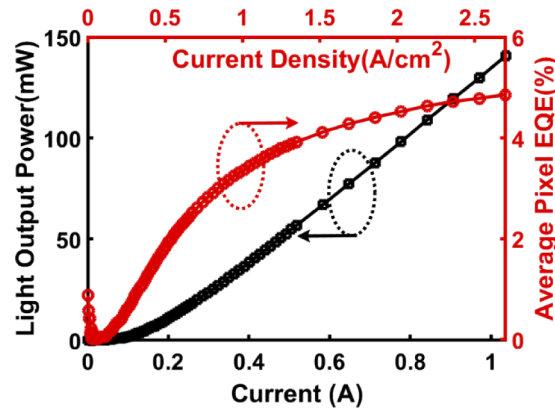


Fig. 4. Light output power (black) and average pixel EQE (red) versus total injection current and current density, using the micro-LED array as a whole for characterization.

As obtained by the integrating sphere measurements, the upper plot of Fig. 5(a) shows the EL spectra of the whole micro-LED array at different injection currents. Full width at half maximum (FWHM) of the EL spectra extends from 17.8 nm to 18.4 nm. The small change in FWHM indicates process uniformity and good heat dissipation capability in this Au-Sn flip-chip bonded micro-display. Peak wavelength shift was also measured as a function of current density. From the lower plot of Fig. 5(a), the peak wavelength decreases from 448.2 nm to 446.6 nm with current density increasing from 0.135 A/cm² to 2.7 A/cm². This blue shift in peak wavelength is caused by the shielding of polarized electric field in associated quantum confined stark effect

(QCSE). The measured data in low current density level, within the driver capability ($J < 1.35$ A/cm² or $I < 500$ mA), can be well fitted by an exponential curve, as shown in the figure, where λ , J are peak wavelength and current density, respectively. a , b and λ_0 are the fitting parameters. The coefficient of determination (R^2) is larger than 0.94. Figure 5(b) shows the CIE1976 (u' , v') coordinates of this blue monochromatic GaN-on-Si micro-LED display. Under normal operation condition (0.675 A/cm²), the CIE (u' , v') coordinates are (0.2114, 0.0671), corresponding to CIE (x , y) coordinates of (0.156, 0.022). When current density increases from 0.135 A/cm² to 2.7 A/cm², the coordinates (u' , v') in Fig. 5(b) move from (0.2184, 0.0784) to (0.2122, 0.0643), where the coordinates' shifting locus (red curve in the inset) stays below sRGB blue and NTSC blue. The color difference of the panel $\Delta u'v'$ was calculated as 0.0153, indicating a less obvious color deviation over the large measured current variation. The deep blue emission, with CIE_y far less than standard blue (sRGB or NTSC), suggests the potential that a larger color gamut can be realized for micro-LEDs implemented in down-conversion full-color display [31].

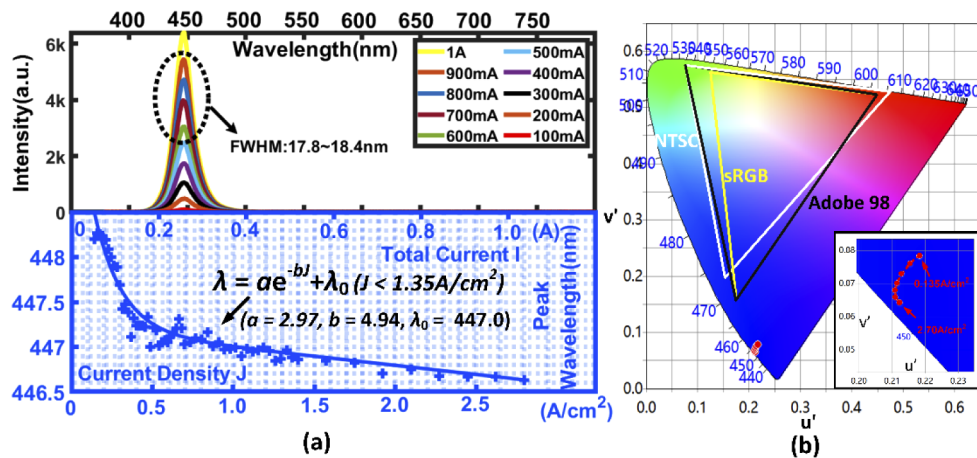


Fig. 5. (a) Top subplot: EL spectra of the whole micro-LED array; bottom subplot: peak wavelength shift as a function of total injection current and its corresponding fitting equation in terms of current density. (b) CIE1976 chromaticity diagram of the micro-LED display; The inset shows coordinates' shifting locus under various current densities.

To measure the luminance performance of this GaN-on-Si micro-LED display, a Photoresearch spectroradiometer was used to characterize the panel brightness. Figure 6(a) shows the measurement setup, in which the digital DC power supply powering the micro-LED display panel was recorded while the spectroradiometers collected the light emitting from the rotating micro-LED chip (in θ direction) with data sent to the computer for post-processing. Figure 6(b) presents the brightness and luminous efficacy of radiation (LER) [32] of the fully powered-on micro-LED array as a function of current density. The panel brightness increases from 0.01 cd/m² to 13337.3 cd/m² with the increased current density from 0 to 2.7 A/cm², leading to the maximum measured contrast larger than 1.06×10^6 in visually dark environment. At half-load and full-load condition, corresponding to a current density of 0.675 A/cm² and 1.35 A/cm², the display panel brightness are 3732.1 cd/m² and 8292.4 cd/m², respectively. Contrast ratios are calculated to be 3.0×10^5 and 6.6×10^5 . The LER of this blue monolithic micro-LED display is around 36 lm/W, which keeps constant over the measured current range, proving the small variance in peak wavelength. Single-pixel luminous power and optical power can therefore be calculated as 10.6 μ lm and 0.29 μ W, respectively, at half load condition with panel luminance of 3732.1 cd/m². In full-color micro-LED display, LER is an important factor to help determine the RGB subpixel power and then operation point for different luminance requirements [32] in the

design process. Compared to those reported high-brightness OLED micro-displays [33,34], this GaN-on-Si micro-LED display shows higher luminance performance, which is also comparable to those GaN-on-sapphire micro-LED display [7]. To further investigate the angular dependence of brightness, the display chip was rotated from 10° to 170° by steps of 10° to measure the luminance distribution as a function of viewing angle. The radiant patterns at different injection currents show a similar and uniform profile, achieving a viewing angle around 120° , as shown in Fig. 6(c).

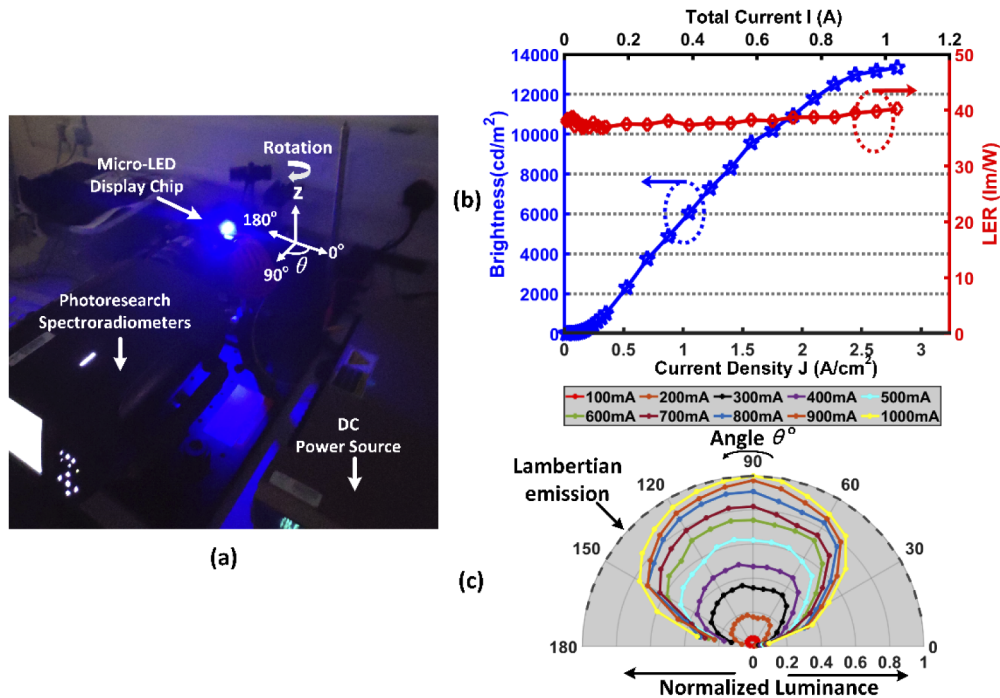


Fig. 6. (a) Measurement setup of luminance and luminous efficacy of radiation (LER) of the micro-LED display. (The spectroradiometer model used for characterization is the Photoresearch PR-655 SpectraScan.) (b) Brightness (blue) and LER (red) of this micro-LED display panel at different current densities. (c) The far-field luminance distribution of the micro-LED display versus viewing angles under various injection currents.

3.3. Demonstration

Figure 7 shows the demonstration setup of this micro-LED display system for direct-view application operating in an indoor direct-view environment. A custom-designed FPGA control board integrated with a micro-SD card reader is used to generate a clock signal and handle the timing sequence. An external small power pack is used to power the FPGA board via an onboard USB interface. Images/videos data are stored in binary files in the micro-SD card and read out by the on-board MCU, then delivered to the column and row drivers through a flexible cable. Compared to the two-transistor one-capacitor (2T1C) driving scheme, the pixel driver in this design adopts a three-transistor one-capacitor (3T1C) scheme [15], achieving 4-bit grayscale display by controlling the pulse width modulation (PWM) frames applied to the additional transistor. To demonstrate display images, original real RGB full-color images with the resolution of 400×240 were first transformed to grayscale images and encoded into binary files by MATLAB. Figure 8 presents grayscale images and their corresponding display images.

The display images are clearly rendered with details, indicating the high yield of this GaN-on-Si micro-LED display. 10 frames per second (fps) videos were successfully demonstrated, showing the high-brightness property. Table 1 summarizes this GaN-on-Si micro-LED display in terms of the display, optical and electrical specifications. To the best of our knowledge, this is the first high-resolution micro-LED display using GaN-on-Si epi-wafer, showing brightness up to 8300 cd/m².



Fig. 7. Setup of the micro-LED display system operating in a high-brightness environment.



Fig. 8. Original grayscale images and their corresponding display images.

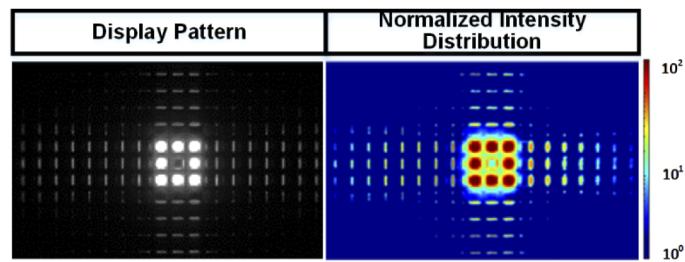
3.4. Discussion and future work

We successfully demonstrated a high-resolution high-brightness GaN-on-Si micro-LED micro-display, with potential for low-cost and large-scale manufacturing. To further improve the display quality, existing optical crosstalk in this micro-display should be taken into account. For this

Table 1. Summary of display performance of the micro-LED display system.

Category	Item	Result
Display Specifications	Substrate	4-inch GaN-on-Si
	Device	Micro-LED
	Pixel size	20 μm \times 20 μm
	Pixel density	400 \times 240
	Active area	0.384 cm^2
	Display size	0.55 inch
Optical Specifications	Brightness	8300 cd/m^2
	Contrast ratio	6.6×10^5
	Grayscale	4-bit
	CIE coordinates (x, y)	(0.156, 0.022)
Electronic Specifications	Driving circuits	CMOS
	Power supply	5 V
	Power consumption	1.17 W (under all-pixels powered-on, full-load condition)
	Refresh rates	100 Hz

monochromatic GaN-on-Si display, reducing optical crosstalk can lead to higher display local contrast. For full-color display using the color-conversion method, such as QDs-based color conversion scheme which features the advantages of high color purity, narrow FWHM [35] and ease for monolithic integration [36,37], optical crosstalk reduction is also important for color gamut improvement. Figure 9 depicts the existing crosstalk issue, in which the powered-on pixel at grayscale of 15 significantly influences the grayscale of adjacent pixels, especially the one in the middle. This is caused by the sidewall emission and $\text{Al}_x\text{Ga}_{1-x}\text{N}$ buffer remained in this non-isolated common cathode structure. To eliminate the optical crosstalk, a complete isolation trench should be implemented between each pixel, and light-absorbing material, such as black matrix, is needed for sidewall passivation. With isolation trenches and light-absorbing passivation layer, the light will be confined within each individual pixel, and thus will not affect the grayscale of its adjacent pixels. We could therefore expect higher local contrast, as well as color gamut improvement in full-color micro-LED displays using the color down-conversion scheme.

**Fig. 9.** Existing optical crosstalk issue in this GaN-on-Si micro-LED display.

4. Conclusions

In conclusion, a 0.55-inch high-brightness 400 \times 240 active matrix GaN-on-Si micro-LED display featuring a pixel size of 20 μm and a pixel pitch of 30 μm was designed, fabricated, and

demonstrated. The micro-LED chip was integrated with a CMOS driver through Au-Sn flip-chip bonding technique, showing a pixel yield larger than 95%. The Si growth substrate was removed by a crack-free wet etching method. Measurement results show the display has a maximum average pixel EQE of 4% and LOP of 54.9 mW at a current density of 1.35 A/cm², limited by the driver capability. FWHM is around 18.2 nm and peak wavelength variation is 1.6 nm, indicating a consistent emission wavelength. The color difference $\Delta u'v'$ is 0.0153 over the measured range from 0.135 A/cm² to 2.7 A/cm² and CIE (*x*, *y*) coordinates of this micro-LED display are located at (0.156, 0.022) when driving at forward voltage, realizing deep blue emission with CIE_y far less than the NTSC blue. The brightness reaches up to 8300 cd/m² under full-load condition, leading to a contrast ratio of 6.6×10^5 . With the control of the PWM frame generated by the FPGA board, we successfully demonstrated 4-bit grayscale images and videos rendering on the display panel. The display contrast could be further improved by the incorporation of isolation trenches into the micro-LED array design and process to completely eliminate the crosstalk issue. This high-brightness, high-resolution micro-LED display demonstration provides a cost-effective and practical solution to micro-displays used in VR/AR applications, circumventing the bottleneck in the development of long-lifespan, high-brightness OLED devices.

Funding. Innovation and Technology Fund (ITS/382/17FP).

Acknowledgments. The authors would like to thank the NFF and Epack of HKUST for technical support. Helpful discussions with Bryan S. T. Tam are also acknowledged.

Disclosures. The authors declare no conflicts of interest.

References

1. M. S. Islam, R. X. Ferreira, X. He, E. Xie, S. Videv, S. Viola, S. Watson, N. Bamiedakis, R. V. Penty, I. H. White, and A. E. Kelly, "Towards 10 Gb/s orthogonal frequency division multiplexing-based visible light communication using a GaN violet micro-LED," *Photonics Res.* **5**(2), A35–A43 (2017).
2. J. F. C. Carreira, E. Xie, R. Bian, C. Chen, J. J. D. McKendry, B. Guilhabert, H. Haas, E. Gu, and M. D. Dawson, "On-chip GaN-based dual-color micro-LED arrays and their application in visible light communication," *Opt. Express* **27**(20), A1517–A1528 (2019).
3. P. Tian, X. Liu, S. Yi, Y. Huang, S. Zhang, X. Zhou, L. Hu, L. Zheng, and R. Liu, "High-speed underwater optical wireless communication using a blue GaN-based micro-LED," *Opt. Express* **25**(2), 1193–1201 (2017).
4. A. Nakajima, H. Kimura, Y. Sawadsaringkarn, Y. Maezawa, T. Kobayashi, T. Noda, K. Sasagawa, T. Tokuda, Y. Ishikawa, S. Shiosaka, and J. Ohta, "CMOS image sensor integrated with micro-LED and multielectrode arrays for the patterned photostimulation and multichannel recording of neuronal tissue," *Opt. Express* **20**(6), 6097–6108 (2012).
5. B. McGovern, R. B. Palmieri, N. Grossman, E. M. Drakakis, V. Poher, M. A. A. Neil, and P. Degenaar, "A new individually addressable micro-LED array for photogenetic neural stimulation," *IEEE Trans. Biomed. Circuits Syst.* **4**(6), 469–476 (2010).
6. V. Poher, N. Grossman, G. T. Kennedy, K. Nikolic, H. X. Zhang, Z. Gong, E. M. Drakakis, E. Gu, M. D. Dawson, P. M. W. French, P. Degenaar, and M. A. A. Neil, "Micro-LED arrays: a tool for two-dimensional neuron stimulation," *J. Phys. D: Appl. Phys.* **41**(9), 094014 (2008).
7. L. Zhang, F. Ou, W. C. Chong, Y. Chen, and Q. Li, "Wafer-scale monolithic hybrid integration of Si-based IC and III-V epi-layers—A mass manufacturable approach for active matrix micro-LED micro-displays," *J. Soc. Inf. Disp.* **26**(3), 137–145 (2018).
8. C. M. Kang, D. J. Kong, J. P. Shim, S. Kim, S. B. Choi, J. Y. Lee, J. H. Min, D. J. Seo, S. Y. Choi, and D. S. Lee, "Fabrication of a vertically-stacked passive-matrix micro-LED array structure for a dual color display," *Opt. Express* **25**(3), 2489–2495 (2017).
9. D. M. Geum, S. K. Kim, C. M. Kang, S. H. Moon, J. Kyhm, J. Han, D. S. Lee, and S. Kim, "Strategy toward the fabrication of ultrahigh-resolution micro-LED displays by bonding-interface-engineered vertical stacking and surface passivation," *Nanoscale* **11**(48), 23139–23148 (2019).
10. H. S. El-Ghoroury, C. L. Chuang, and Z. Y. Alpaslan, "26.1: Invited Paper: Quantum Photonic Imager (QPI): A Novel Display Technology that Enables more than 3D Applications," *Dig. Tech. Pap. - Soc. Inf. Disp. Int. Symp.* **46**(1), 371–374 (2015).
11. J. Park, J. H. Choi, K. Kong, J. H. Han, J. H. Park, N. Kim, E. Lee, D. Kim, J. Kim, D. S. Chung, and M. Kim, "Electrically driven mid-submicron pixelation of InGaN micro-LED displays for AR glasses," *Research Square* (2021).
12. Y. Huang, E. L. Hsiang, M. Y. Deng, and S. T. Wu, "Mini-LED, Micro-LED and OLED displays: Present status and future perspectives," *Light: Sci. Appl.* **9**(1), 1–16 (2020).

13. Z. J. Liu, W. C. Chong, K. M. Wong, and K. M. Lau, "360 PPI flip-chip mounted active matrix addressable light emitting diode on silicon (LEDoS) micro-displays," *J. Disp. Technol.* **9**(8), 678–682 (2013).
14. W. C. Chong, W. K. Cho, Z. J. Liu, C. H. Wang, and K. M. Lau, "1700 pixels per inch (PPI) passive-matrix micro-LED display powered by ASIC," *IEEE Compound Semiconductor Integrated Circuit Symposium (CSICS)*, 1–4 (2014).
15. X. Li, L. Wu, Z. Liu, B. Hussain, W. C. Chong, K. M. Lau, and C. P. Yue, "Design and characterization of active matrix LED microdisplays with embedded visible light communication transmitter," *J. Lightwave Technol.* **34**(14), 3449–3457 (2016).
16. J. Day, J. Li, D. Y. C. Lie, C. Bradford, J. Y. Lin, and H. X. Jiang, "III-Nitride full-scale high-resolution microdisplays," *Appl. Phys. Lett.* **99**(3), 031116 (2011).
17. J. Day, J. Li, D. Y. C. Lie, C. Bradford, J. Y. Lin, and H. X. Jiang, "Full-scale self-emissive blue and green microdisplays based on GaN micro-LED arrays," *Proc. SPIE* **8268**, 82681X (2012).
18. F. Templier, L. Dupré, B. Dupont, A. Daami, B. Aventurier, F. Henry, D. Sarrasin, S. Renet, F. Berger, F. Olivier, and L. Mathieu, "High-resolution active-matrix 10-um pixel-pitch GaN LED microdisplays for augmented reality applications," *Proc. SPIE* **10556**, 105560I (2018).
19. F. Templier, "GaN-based emissive microdisplays: A very promising technology for compact, ultra-high brightness display systems," *J. Soc. Inf. Disp.* **24**(11), 669–675 (2016).
20. C. J. Chen, H. C. Chen, J. H. Liao, C. J. Yu, and M. C. Wu, "Fabrication and Characterization of Active-Matrix 960 × 540 Blue GaN-Based Micro-LED Display," *IEEE J. Quantum Electron.* **55**(2), 1–6 (2019).
21. A. Nishikawa, A. Loesing, and B. Slischka, "Invited Paper: Achieving high uniformity and yield of 200 mm GaN-on-Si LED epiwafers for micro LED applications with precise strain-engineering," *Dig. Tech. Pap. - Soc. Inf. Disp. Int. Symp.* **50**(1), 338–341 (2019).
22. Plessey, "AR-Vμ™," <https://plesseysemiconductors.com/microleds/active-matrix-display/>
23. X. Zhang, P. Li, X. Zou, J. Jiang, S. H. Yuen, C. W. Tang, and K. M. Lau, "Active matrix monolithic LED micro-display using GaN-on-Si epilayers," *IEEE Photonics Technol. Lett.* **31**(11), 865–868 (2019).
24. S. C. Huang, H. Li, Z. H. Zhang, H. Chen, S. C. Wang, and T. C. Lu, "Superior characteristics of microscale light emitting diodes through tightly lateral oxide-confined scheme," *Appl. Phys. Lett.* **110**(2), 021108 (2017).
25. C. C. Li, J. L. Zhan, Z. Z. Chen, F. Jiao, Y. F. Chen, Y. Y. Chen, J. X. Nie, X. N. Kang, S. F. Li, Q. Wang, and G. Y. Zhang, "Operating behavior of micro-LEDs on a GaN substrate at ultrahigh injection current densities," *Opt. Express* **27**(16), A1146–A1155 (2019).
26. A. Daami, F. Olivier, L. Dupré, F. Henry, and F. Templier, "Invited Paper: Electro-optical size-dependence investigation in GaN micro-LED devices," *Dig. Tech. Pap. - Soc. Inf. Disp. Int. Symp.* **49**(1), 790–793 (2018).
27. P. Tian, J. J. McKendry, Z. Gong, B. Guilhabert, I. M. Watson, E. Gu, Z. Chen, G. Zhang, and M. D. Dawson, "Size-dependent efficiency and efficiency droop of blue InGaN micro-light emitting diodes," *Appl. Phys. Lett.* **101**(23), 231110 (2012).
28. F. Olivier, S. Tirano, L. Dupré, B. Aventurier, C. Largeton, and F. Templier, "Influence of size-reduction on the performances of GaN-based micro-LEDs for display application," *J. Lumin.* **191**, 112–116 (2017).
29. M. S. Wong, D. Hwang, A. I. Alhassan, C. Lee, R. Ley, S. Nakamura, and S. P. DenBaars, "High efficiency of III-nitride micro-light-emitting diodes by sidewall passivation using atomic layer deposition," *Opt. Express* **26**(16), 21324–21331 (2018).
30. S. Zhou, H. Xu, B. Tang, Y. Liu, H. Wan, and J. Miao, "High-power and reliable GaN-based vertical light-emitting diodes on 4-inch silicon substrate" *Opt.* *Opt. Express* **27**(20), A1506–A1516 (2019).
31. X. Zhang, L. Qi, W. C. Chong, P. Li, C. W. Tang, and K. M. Lau, "Active matrix monolithic micro-LED full-color micro-display," *J. Soc. Inf. Disp.* **29**(1), 47–56 (2021).
32. J. J. Wierer Jr and N. Tansu, "III-Nitride Micro-LEDs for Efficient Emissive Displays," *Laser Photonics Rev.* **13**(9), 1900141 (2019).
33. A. Ghosh, E. P. Donoghue, I. Khayrullin, T. Ali, I. Wacyk, K. Tice, F. Vazan, L. Sziklas, D. Fellowes, and R. Draper, "Invited Paper: Directly Patterened 2645 PPI Full Color OLED Microdisplay for Head Mounted Wearables," *Dig. Tech. Pap. - Soc. Inf. Disp. Int. Symp.* **47**(1), 837–840 (2016).
34. A. Ghosh, E. P. Donoghue, I. Khayrullin, T. Ali, L. Wacyk, K. Tice, F. Vazan, O. Prache, Q. Wang, L. Sziklas, and D. Fellowes, "Invited Paper: Ultra-High-Brightness 2 K × 2 K Full-Color OLED Microdisplay Using Direct Patterning of OLED Emitters," *Dig. Tech. Pap. - Soc. Inf. Disp. Int. Symp.* **48**(1), 226–229 (2017).
35. C. H. Lin, A. Verma, C. Y. Kang, Y. M. Pai, T. Y. Chen, J. J. Yang, C. W. Sher, Y. Z. Yang, P. T. Lee, C. C. Lin, Y. C. Wu, S. K. Sharma, T. Wu, S. R. Chung, and H. C. Kuo, "Hybrid-type white LEDs based on inorganic halide perovskite QDs: candidates for wide color gamut display backlights," *Photonics Res.* **7**(5), 579–585 (2019).
36. X. Zhang, L. Qi, W. C. Chong, P. Li, and K. M. Lau, "23-5: Late-News Paper: High-Resolution Monolithic Micro-LED Full-color Micro-display," *Dig. Tech. Pap. - Soc. Inf. Disp. Int. Symp.* **51**(1), 339–342 (2020).
37. S. W. H. Chen, Y. M. Huang, K. J. Singh, Y. C. Hsu, F. J. Liou, J. Song, J. Choi, P. T. Lee, C. C. Lin, Z. Chen, J. Han, T. Wu, and H. C. Kuo, "Full-color micro-LED display with high color stability using semipolar (20-21) InGaN LEDs and quantum-dot photoresist," *Photonics Res.* **8**(5), 630–636 (2020).